Ferromagnetic Bonding: Properties of High-Spin Lithium Clusters $^{n+1}Li_n$ ($n = 2-12$) Devoid of Electron Pairs

Sam P. de Visser,[†] David Danovich,[†] Wei Wu,[‡] and Sason Shaik*,[†]

The Department of Organic Chemistry and the Lise Meitner-Minerva Center for Computational Quantum Chemistry, The Hebrew University of Jerusalem, 91904 Jerusalem, Israel, and The Department of Chemistry and the State Key Laboratory for Physical Chemistry of Solid Surfaces, Xiamen University, Xiamen, Fujian 361005, Peoples Republic of China

Received: December 31, 2001

Density functional calculations are used to generate a series of the maximum-spin lithium clusters $^{n+1}Li_n$ (n=2−12). These clusters do not possess any electron pairs and have formally a bond order of zero but are nevertheless strongly bound by what we describe here as "ferromagnetic bonding" (FM bonding). The FM bonding energy rises from 1.7 kcal mol^{-1} for the dimer to 145 kcal mol^{-1} for the dodecamer, and the bond energy per atom converges for cluster sizes of $n = 11-12$ reaching values of 11−12 kcal mol^{-1} atom^{-1}. In line with previous studies of such clusters (*Isr. J. Chem.* **1993**, *33*, 455; *J. Phys. Chem. A* **2000**, *104*, 11223), FM bonding is found to prefer highly symmetrical egg-shaped structures with a high coordination number for the Li atom. The mechanism of FM bonding is elucidated using a valence bond (VB) model equation and an orbital picture, which are projected from previous detailed calculations of the $^3Li_2$ dimer (*J. Am. Chem. Soc.* **1999**, *121*, 3165). The VB model is shown to capture the essence of FM bonding. Thus, the shape of the cluster, its steeply rising bond energy, and the convergence of the bonding energy per single atom all find a simple rationale in the VB model. It turns out that FM bonding is a delocalized covalent−ionic fluctuation that spreads over the entire cluster. This unique bonding type is likely to manifest also in clusters of noble elements. The strong bonding and high-spin state suggest that such clusters should have a long enough lifetime to be observed.

1. Introduction

Clusters constitute the intermediate situation between the isolated molecular state and the condensed macroscopic state.[1−8] Some of the fundamental properties which one would like to understand about clusters are their binding energy, the nature of the bonding mechanism, and its asymptotic behavior as the cluster grows to its macroscopic limit. This paper deals with the bonding mechanism that holds together maximum-spin species, which are devoid of electron pairs but nevertheless are strongly bonded. Such clusters are the maximum-spin lithium clusters, $^{n+1}Li_n$, dubbed "no-pair" clusters[9] and described recently by theoretical means.[9−11] They are however not a mere theoretical curiosity since very recently, the "no-pair" $^3Cs_2$ ($^3\Sigma_u^+$) dimer was probed by experimental photoassociation spectroscopy and found to be weakly bound[12] relative to the two separated ground state atoms. As shown here, the binding energy of these clusters rises steeply with the cluster size and reaches values of as much as 12 kcal mol^{-1} per lithium atom! With these binding energies, it is clear that one is not dealing with weak van der Waals interactions but rather with "ferromagnetic bonds" which sustain large clusters with maximum magnetization. It is important therefore to develop a bonding model that provides insight into this novel ferromagnetic bonding (FM bonding) and can predict the bonding energies of these clusters as the cluster size increases.

Most of the studies of lithium clusters, by experimental and theoretical means,[13−24] focused on the ground state which is low-spin and bonded by electron pairing. To the best of our knowledge, the possible existence of bonded high-spin clusters was pointed out for the first time by McAdon and Goddard,[16−18] who used generalized valence bond (GVB) and showed that the ring structure $^{11}Li_{10}$ is bound and exhibits singly occupied interstitial orbitals which are ferromagnetically coupled. A systematic study of "no-pair" high-spin $^{n+1}Li_n$ clusters up to $^7Li_6$ was taken by Glukhovtsev and Schleyer[9] who stressed the substantial binding energy and the symmetric geometries of these clusters. Subsequently,[10] we confirmed these trends at the coupled cluster CCSD(T) level and used the multistructure breathing orbital valence bond (BOVB) method[25] to investigate the origins of bonding in the triplet lithium dimer in its $^3\Sigma_u^+$ state ($\sigma_g^1\sigma_u^1$ configuration). We initially ascertained that neither the Hartree−Fock nor the GVB levels gave any bonding for the dimer, and it is only the flexibility of the multistructure VB wave function that could reproduce the CCSD(T) result.

The VB computations[10] showed that FM bonding is sustained by resonance mixing of the repulsive $2s_A^1 2s_B^1$ triplet structure with corresponding charge transferred and locally excited structures which endow the no-pair dimer with resonance energy stabilization due to the covalent-ionic fluctuation of the triplet pair. When the dimer results were projected, it was possible to derive a general expression for the cluster binding energy as a function of the cluster size, on the basis of the resonance mixing of the repulsive 2s-only structure with the locally excited and charge transfer structures. The VB model could also predict that the no-pair clusters have a propensity to aggregate in highly

* To whom correspondence should be addressed. FAX: +972-2-6584680. E-mail: sason@yfaat.ch.huji.ac.il.
† The Hebrew University of Jerusalem.
‡ Xiamen University.

10.1021/jp014665e CCC: $22.00
Published on Web 04/20/2002

TABLE 1: Bond Dissociation Energies (BDE) and Geometric Parameters of Different $^8Li_7$ and $^9Li_8$ Minima Calculated at Different Levels of Theory

		B3PW91		B3P86		UCCSD(T)
entry	isomer[a]	BDE (kcal mol^{-1})	bond distance(s) (Å)	BDE (kcal mol^{-1})	bond distance(s) (Å)	BDE (kcal mol^{-1})
$^8Li_7$						
1	linear $^8\Sigma_u$; $D_{\infty h}$[b]	30.1	3.310; 3.231; 3.223	33.9	3.279; 3.206; 3.199	22.2
2	cyclo $^8A_1'$; D_{7h}	46.5	3.184	51.3	3.158	51.7
3	pyramid $^8A_1$; C_{6v}[c]	48.2	3.116; 3.109	54.3	3.067; 3.056	51.5
4	flower [**1**] $^8A_1$; C_{3v}	53.0	Figure 1	58.8	Figure 1	54.7
5	tower [**2**] $^8A_1$; C_{3v}	58.0	Figure 1	63.8	Figure 1	60.0
$^9Li_8$						
6	linear $^9\Sigma_g$, $D_{\infty h}$[d]	37.6	3.307; 3.231; 3.225; 3.225	42.2	3.277; 3.206; 3.200; 3.201	30.0
7	cyclo $^9B_{2g}$, D_{8h}	39.4	3.089	60.5	3.169	61.2
8	Napoleon's hat [**3**] $^9B_2$, C_{2v}	68.8	Figure 1	75.6	Figure 1	71.4
9	dodecahedron [**4**] $^9B_2$, D_2	73.6	Figure 1	80.4	Figure 1	77.5

[a] Following each isomer are written the structure number in Figure 1 (in square brackets) and the electronic state and symmetry group. [b] Order of bond distances is r_{12}, r_{23}, and r_{34}. [c] Order of bond distances is r_{12} and r_{23}. [d] Order of bond distances is r_{12}, r_{23}, r_{34}, and r_{45}.

symmetric geometries, which maximize the coordination number of the atoms and possess uniform Li−Li distances. Thus, the VB model provides potentially a basis for understanding the root cause of FM bonding and for predicting its asymptotic behavior at infinite cluster size.[10]

The predictions of the VB model require testing on larger and larger clusters, which are beyond the capabilities of BOVB multistructure computations. Following our recent study[11] that established the reliability of density functional theoretic (DFT) calculations, for $^{n+1}Li_n$ ($n = 2-6$), the present paper uses DFT to study larger clusters up to the point where the binding energy per atom converges. The binding energies and geometries are compared with the predictions of the VB model for FM bonding. It is shown that FM bonding is a covalent−ionic fluctuation that spreads over the entire cluster. This bonding paradigm may have general application beyond lithium clusters.

2. Theoretical Methods

Density Functional Methods. All calculations presented here were performed with the Gaussian 98 package.[26] For each cluster size, $^{n+1}Li_n$ ($n = 7-12$), a complete geometry optimization was carried out for different point group symmetries, going from the highest symmetry down to C_1 symmetry. This was followed by complete frequency analyses. Compact geometries with a maximum amount of interatomic bonds were tested, alongside the linear and cyclic isomers which invariably proved to be local minima for $^{n+1}Li_n$ ($n = 3-6$).[11] Thus, although we did not exhaust all of the possible isomers for a given cluster size, we tested enough of them to offer some generalizations. For comparison, we tested also isomers for the lowest spin state vis-à-vis the high spin structures to verify that the choice of the most stable cluster is indeed different for the two spin situations. The calculations were done using Becke's three parameter exchange functional[27] in combination with correlation functionals from either Perdew (P86)[28] or Perdew and Wang (PW91)[29] with a cc-pVDZ basis set,[30−32] hence, B3P86/cc-pVDZ and B3PW91/cc-pVDZ, respectively. These hybrid functionals were shown to give results at par with CCSD(T)/cc-pVDZ.[11]

In all situations, it was ascertained that doubly occupied orbitals are core 1s orbitals. In the cases of $^8Li_7$ and $^9Li_8$ single-point UCCSD(T)/cc-pVDZ calculations were done on B3P86/cc-pVDZ optimized geometries. These UCCSD(T) values serve as an additional benchmark for the DFT methods. All of the data is summarized as a Gaussian archive form in the Supporting Information deposited with this paper. In the text, we discuss only the results for the most stable clusters and for the other genuine structural minima.

Other Theoretical Methods. Tests of GVB and Hartree−Fock (HF) levels were carried on the $^3\Sigma_u^+$ state of Li_2 for which both gave a repulsive state. CASSCF calculations gave a bonded state but with a smaller bonding energy compared with the benchmark CCSD(T) level.[10] The multistructure BOVB result was, on the other hand, in accord with the benchmark method, thus highlighting the importance of both static and dynamic electron correlation for FM bonding. On $^4Li_3$, HF theory gave a negligible bond dissociation energy as was noted already in ref 9. GVB too underestimated the bonding energy for $^4Li_3$ (2.8 kcal mol^{-1} compared with 11.0 kcal mol^{-1}).[10]

3. Results

In what follows, the bond dissociation energy (BDE) is defined as the dissociation energy of a cluster (Li_n) into n individual atoms in their ground states. The relative bond dissociation energy (BDE/n) is defined as the bond dissociation energy per single lithium atom. BDEs and critical geometric parameters for a selection of the optimized $^{n+1}Li_n$ ($n = 7-12$) clusters are collected in Tables 1 and 2. Figures 1 and 2 depict the lowest energy structures. All structures presented in Tables 1 and 2 correspond to minima confirmed by frequency analysis.

The Most Stable Isomers. The lowest energy $^8Li_7$ structure, among those tested, is the tower (**2**) with C_{3v} symmetry and bond dissociation energies of 58.0 (B3PW91) and 63.8 kcal mol^{-1} (B3P86). The "flower" isomer (**1**), also with C_{3v} symmetry, was found to be a local minimum 5.0 kcal mol^{-1} higher in energy than the "tower". A close contender to the four lowest isomers is the "pyramid" (entry 3 in Table 1) with a C_{6v} symmetry. The central lithium atom in the pyramidal structure is only 0.198 (B3PW91) and 0.264 Å (B3P86) above the plane of the remaining six lithium atoms, and the two geometrical degrees of freedom are very close to each other resulting in an almost planar structure. Interestingly, the planar D_{6h} symmetrical isomer has virtually the same energy as the pyramidal configuration but is a second-order saddle point at the B3PW91 level of theory and a first-order saddle point at the B3P86 level of theory (see the Supporting Information). The most stable $^9Li_8$ isomer is the dodecahadron **4** in Figure 1, although **3** is a close contender. For both $^8Li_7$ and $^9Li_8$, all other tested geometries are high order saddle points (see the Supporting Information).

To test that the DFT results continue to be reliable[11] for the larger clusters, we performed single-point UCCSD(T)/cc-pVDZ

TABLE 2: Energies and Bond Dissociation Energies (BDE) of Different $^{10}Li_9$, $^{11}Li_{10}$, $^{12}Li_{11}$, and $^{13}Li_{12}$ Minima

			B3PW91		B3P86	
entry		isomer[a]	BDE (kcal mol^{-1})	bond distance(s) (Å)	BDE (kcal mol^{-1})	bond distance(s) (Å)
1	$^{10}Li_9$	linear $^{10}\Sigma_g$, $D_{\infty h}$[b]	45.2	3.307; 3.232; 3.226; 3.227	50.5	3.276; 3.207; 3.202; 3.203
2		cyclo $^{10}A_1'$, D_{9h}	63.6	3.203	69.6	3.178
3		rotated diamond [**5**] $^{10}A_2$, C_{2v}	91.9	Figure 2	99.8	Figure 2
4	$^{11}Li_{10}$	linear $^{11}\Sigma_u$, $D_{\infty h}$[c]	49.0	3.016; 3.122; 3.208; 3.228; 3.231	55.1	2.987; 3.097; 3.184; 3.204; 3.207
5		Cyclo $^{11}B_{2u}$, D_{10h}	71.9	3.209	78.6	3.184
6		rotated diamond [**6**] $^{11}B_2$, D_{4d}	108.5	Figure 2	117.4	Figure 2
7	$^{12}Li_{11}$	linear $^{12}\Sigma_u$, $D_{\infty h}$[c]	60.6	3.306; 3.232; 3.227 3.229; 3.231	67.2	3.276; 3.207; 3.202 3.204; 3.206
8		cyclo $^{12}A_1'$, D_{11h}	80.1	3.214	87.6	3.189
9		C_1 structure [**7**] ^{12}A, C_1	121.8	Figure 2	131.8	Figure 2
10	$^{13}Li_{12}$	linear $^{13}\Sigma_g$, $D_{\infty h}$[d]	68.3	3.306; 3.232; 3.227 3.230; 3.231; 3.232	75.6	3.276; 3.207; 3.203 3.205; 3.207; 3.207
11		cyclo $^{13}B_{2g}$, D_{12h}	88.3	3.218	96.4	3.192
12		icosahedral [**8**] ^{13}A, I_h[e]	129.4	Figure 2	140.5	Figure 2
13		egg [**9**] $^{13}A_u$, C_i	133.9	Figure 2	145.1	Figure 2

[a] Following each isomer are written the structure number in Figure 2 (in square brackets) and the electronic state and the point group symmetry. [b] Order of bond distances is r_{12}, r_{23}, r_{34}, and r_{45}. [c] Order of bond distances is r_{12}, r_{23}, r_{34}, r_{45}, and r_{56}. [d] Order of bond distances is r_{12}, r_{23}, r_{34}, r_{45}, r_{56}, and r_{67}. [e] The structure had two imaginary frequencies.

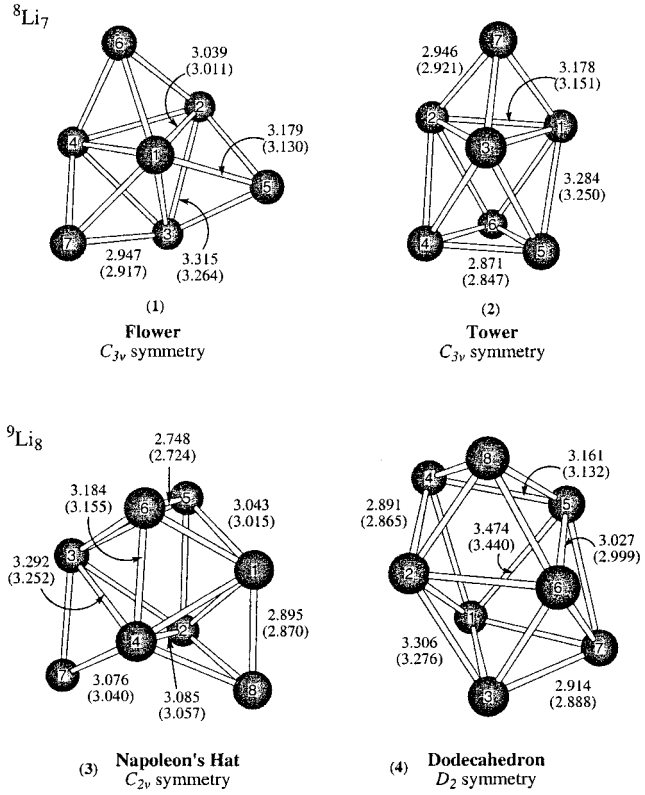

Figure 1. Optimized $^8Li_7$ and $^9Li_8$ structures, with bond distances in Å, calculated by use of B3PW91/cc-pVDZ (out of parentheses) and B3P86/cc-pVDZ (in parentheses).

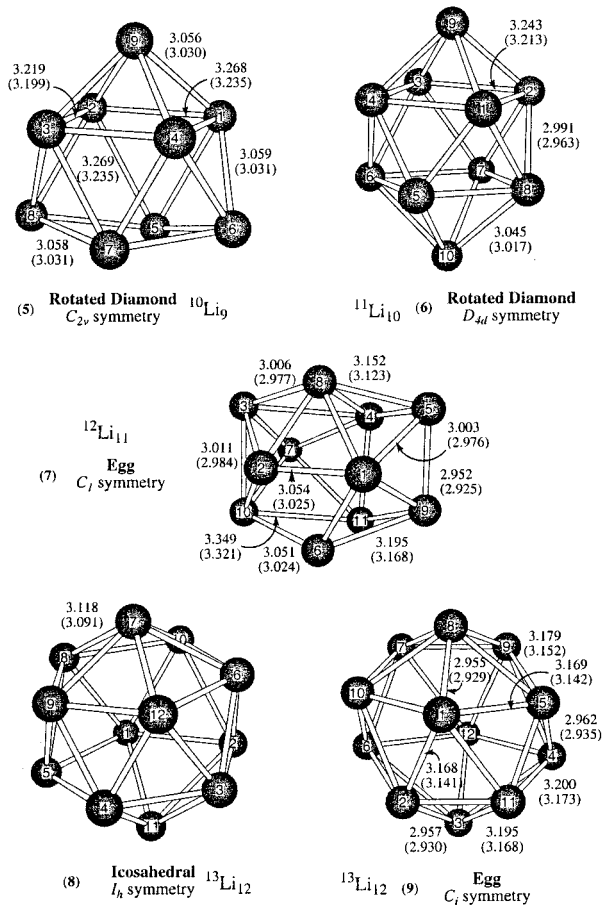

Figure 2. Optimized $^{10}Li_9$, $^{11}Li_{10}$, $^{12}Li_{11}$, and $^{13}Li_{12}$ structures, with bond distances in Å, calculated with B3PW91/cc-pVDZ (out of parentheses) and B3P86/cc-pVDZ (in parentheses).

calculations on a few $^8Li_7$ and $^9Li_8$ isomers (Table 1). For example, the BDE(UCCSD(T)) values for the stable $^8Li_7$ isomers, the "flower" (**1**) and the "tower" (**2**), are 54.7 and 60.0 kcal mol^{-1}, respectively. These values are between B3PW91 and B3P86 (compare with entries 4 and 5 in Table 1). For the "hat" (**3**) and dodecahedron (**4**) isomers of $^9Li_8$, the BDE(UCCSD(T)) results are 71.4 and 77.5 kcal mol^{-1}; again between the corresponding B3PW91 and B3P86 values. The same result was obtained for other $^8Li_7$ and $^9Li_8$ isomers. An exception is the cyclic $^9Li_8$ isomer (entry 7, Table 1) that has very different B3P86 and B3PW91 BDE values, even though both methods converge on the same electronic structure. The BDE(UCCSD(T)) result is 61.2 kcal mol^{-1} within less than 1 kcal mol^{-1} of the B3P86 value. We may conclude therefore that the two DFT methods are reasonably accurate for no-pair clusters, with B3P86 being somewhat better.

Figure 2 shows the most stable $^{10}Li_9$, $^{11}Li_{10}$, $^{12}Li_{11}$, and $^{13}Li_{12}$ isomers (**5**−**9**), and all other local minima are collected in Table 2. The BDE values for the cyclo-$^{11}Li_{10}$ ($^{11}B_{2u}$) are 71.9 (B3PW91) and 78.6 (B3P86). Both are larger than the GVB

SCHEME 1: Kohn−Sham Orbitals of Icosahedral $^{13}Li_{12}$

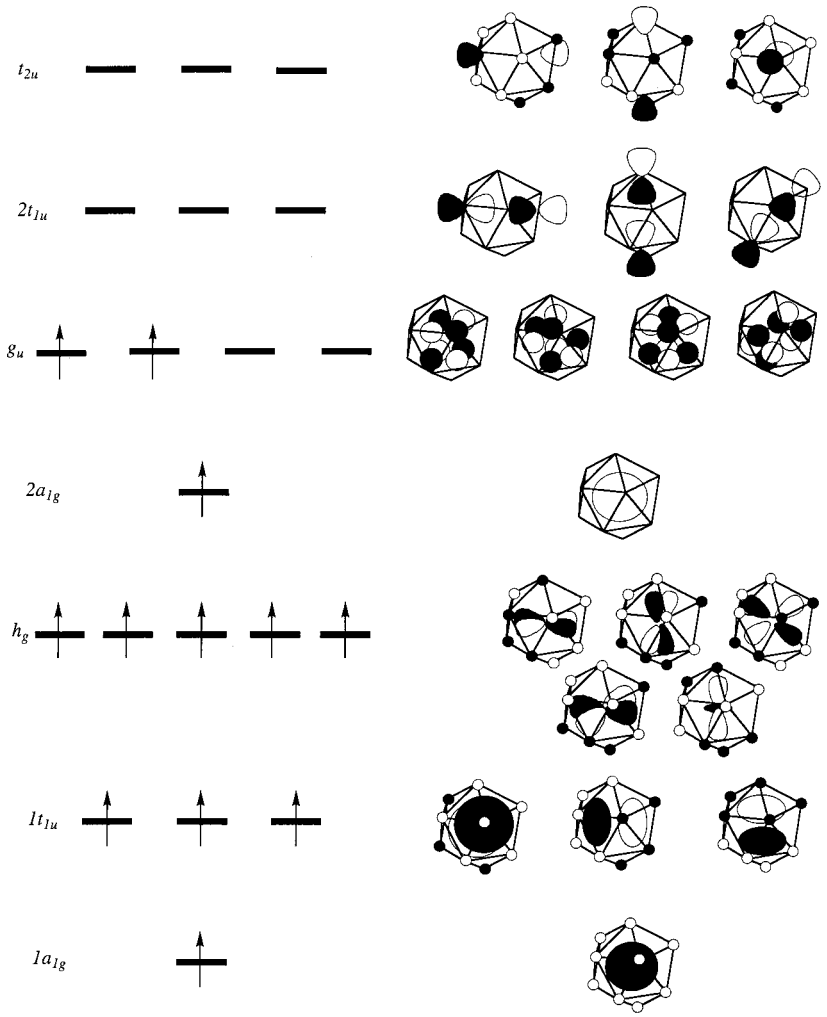

value of 60.7 kcal mol^{-1} calculated by McAdon and Goddard.[16−18] On the basis of the comparison with UCCSD(T) values, the DFT value of $^{11}B_{2u}$ should be between 71.9 and 78.6 kcal mol^{-1}.

The reason the $^{13}Li_{12}$ icosahedron is not the most stable dodecamer emerges by inspecting the Kohn−Sham orbitals of the icosahedron, in Scheme 1. The singly occupied valence orbitals of the icosahedron are built up from 2s and 2p$_\sigma$ type of orbitals. As a consequence, the orbitals have interstitial electron density as shown by McAdon and Goddard for the low-spin clusters.[16−18] In particular, in the icosahedron, there is a large electron density inside the cage. This originates in orbitals locked into the icosahedral cage: a 1s-type orbital which is the lowest $1a_{1g}$ orbital, three 2p-type orbitals which correspond to the $1t_{1u}$ orbitals, and five degenerate singly occupied orbitals (h_g symmetry) with a 3d-shaped orbital. Apart from electron density inside the cage, the $1a_{1g}$, $1t_{1u}$, and h_g orbitals also have a small electron density on the atomic centers, which is absent from the remaining singly occupied orbitals. Thus, the higher lying singly occupied $2a_{1g}$ orbital is made from 2p$_\sigma$ orbitals in a bonding combination, resulting in electron density that is restricted to the inside of the cage. The highest two singly occupied orbitals of the icosahedron in our calculations correspond to two g_u orbitals. Two-electron occupation in the quadruply degenerate g_u set leads to a Jahn−Teller distortion that removes the degeneracy of these orbitals. Therefore, the icosahedron system is not the minimum energy structure but a second-order saddle point. Attempts to bring the three antibonding 2s+2p$_\sigma$ orbitals with t_{2u} symmetry in the active space by removing the highest three singly occupied orbitals with $2a_{1g}$, g_u, and g_u symmetry failed. A geometry optimization starting with the Cartesian coordinates of the icosahedron plus the normal modes of the imaginary frequencies led to the minimum energy structure in C_i symmetry, **9** in Figure 2. Note however, that it is geometrically not very different from the icosahedral isomer. In fact, the "egg" **9** is the slightly distorted form of the icosahedron.

Less Stable Isomers. As indicated above, many local minima have been obtained in this study. In particular, all linear ($D_{\infty h}$ symmetry) and cyclic (D_{nh} symmetry) $^{n+1}Li_n$ clusters in the range between the trimer and the dodecamer are local minima. In general, though, the total bonding energy of the linear and cyclic isomers is much weaker compared with the most stable high spin clusters (Tables 1 and 2).

The relative bond dissociation energy, BDE/n, of the linear lithium clusters is plotted, in Figure 3, as a function of cluster size. For $n/2$ = even (n = even) and ($n - 1$)/2 = even (n = odd) the linear configurations have a $^{n+1}\Sigma_g$ electronic state, whereas a $^{n+1}\Sigma_u$ electronic state is found for $n/2$ = odd (n = even) and ($n - 1$)/2 = odd (n = odd). In addition to the linear structures, the relative bond dissociation energies of cyclic lithium clusters were added to Figure 3. All cyclic isomers with n = odd possess an $^{n+1}A_1'$ electronic state. The lowest high spin state for n = even cyclic isomers is the $^{n+1}B_{2g}$ electronic state for $n/2$ = even, whereas a $^{n+1}B_{2u}$ electronic state is found for $n/2$ = odd.

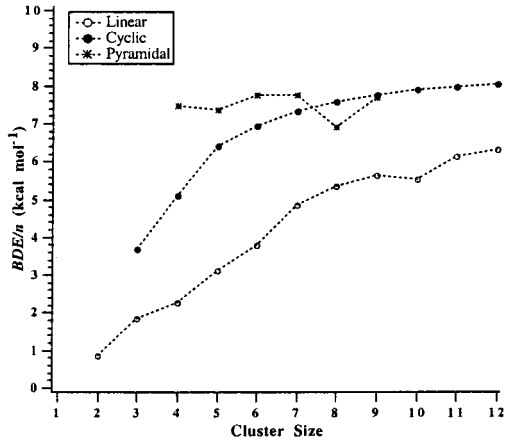

Figure 3. Relative bond dissociation energies (BDE/n) of linear, cyclic, and pyramidal isomers. Data obtained with the B3P86/cc-pVDZ method.

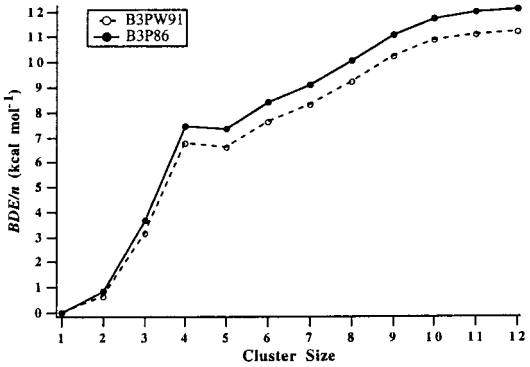

Figure 4. Relative bond dissociation energy (BDE/*n*) of the most stable isomers as a function of the size of the cluster calculated at the B3P86/cc-pVDZ and B3PW91/cc-pVDZ methods.

We recall that the most stable $^5Li_4$ and $^6Li_5$ structures were found[11] to be the pyramidal configurations. The $^7Li_6$ pyramidal structure is still a minimum albeit 4.1 kcal mol^{-1} higher in energy as the most stable pair of structures.[11] The pyramidal $^8Li_7$ structure is a local minimum but considerably higher in energy compared with the most stable structure by 9.5 kcal mol^{-1}. Larger pyramidal clusters are high order saddle points: the $^9Li_8$ structure has two imaginary frequencies, whereas the nonamer has six imaginary frequencies. Consequently, larger pyramidal structures were not investigated. Figure 3 also contains the relative bond dissociation energies (BDE/*n*) of the pyramidal structures in the range between $^5Li_4$−$^{10}Li_9$ as a function of the number of lithium atoms. Remarkably, the BDE/*n* values of the pyramidal structures are almost constant with an average value of 7.6 kcal mol^{-1}. Even more remarkable is the fact that in all isomers a plateau (or nearly so) in BDE/*n* is reached around $^{13}Li_{12}$.

Trends for the Most Stable No-Pair Isomers. Figure 4 gives relative bond dissociation energies as a function of cluster size for the most stable clusters. It is seen that the relative bond dissociation energy reaches a plateau at around 11 or 12 lithium atoms. It may be anticipated that lithium clusters with more than 12 atoms will not show an increase of the relative bond dissociation energy but will stabilize at around 12.1 kcal mol^{-1} (the B3P86 value). Notice as well the small peak for the tetramer caused by the pyramidal geometry, which is ultrastable due probably to its highly symmetric (see discussion) and short Li−Li distances. All other clusters follow a regular increasing trend. The B3PW91 and B3P86 data exhibit the same trends, and the only difference is the plateau value of the BDE/*n* which is 11.2 kcal mol^{-1} with B3PW91. Thus, in fact, all no-pair clusters of different geometrical varieties seem to exhibit a plateau in their relative BDE near $n = 12$ (compare Figures 3 and 4).

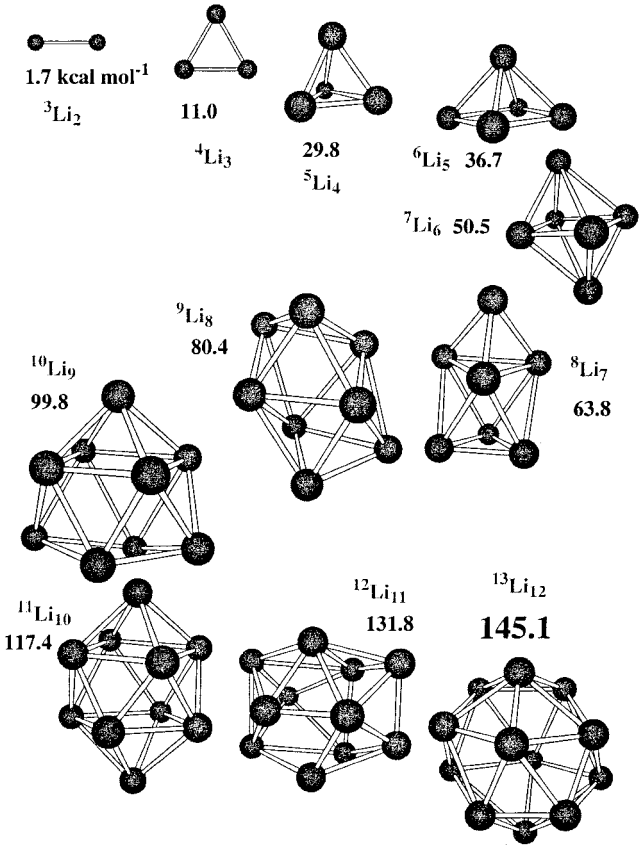

Figure 5. Most stable no-pair clusters and their bonding energy (B3P86/cc-pVDZ) values.

4. Discussion

The foregoing results together with those in previous papers[9−11] span "no-pair" clusters ($^{n+1}Li_n$) in the range between $n = 2-12$. A general picture emerges that enables us to outline trends in these clusters, and to generalize the origins of FM bonding. The discussion is focused at the most stable isomers found in the study.

4.1. Evolution of FM Bonding. The most stable ($^{n+1}Li_n$) isomers are assembled in Figure 5, along with the total bond energy (B3P86/cc-pVDZ), relative to the separated atoms in the ground states. The gradual evolution can be viewed as a sequential capping of a lithium atom to afford the maximum coordination number that increases, from two for $^4Li_3$ to five for $^{13}Li_{12}$. Two trends emerge from the figure: First, the clustering process of the no-pair species forms spherical egg-like objects that are close to completely symmetric structures, which maximize the coordination number of the Li atom. Second, the bond energy of the cluster increases from a meager 1.7 to ca. 145 kcal mol^{-1} for the $^{13}Li_{12}$ cluster (the corresponding B3PW91 data are 0.85 and 134 kcal mol^{-1}). This is a huge bonding energy, for species with a formal bond order of zero and with absolutely no electron pairs. It is apparent that strong chemical bonding is at work here, rather than weak van der Waals forces, as one might have deduced by considering the binding energy of the dimer alone, either in $^3Li_2$ here or in the experimentally probed $^3Cs_2$ dimer.[12] It is appropriate therefore to call this bonding mechanism FM bonding, and distinguish it from the common low-spin electron pair bonding.

SCHEME 2: Principal VB Structures Which Account for FM bonding in $^3Li_2$

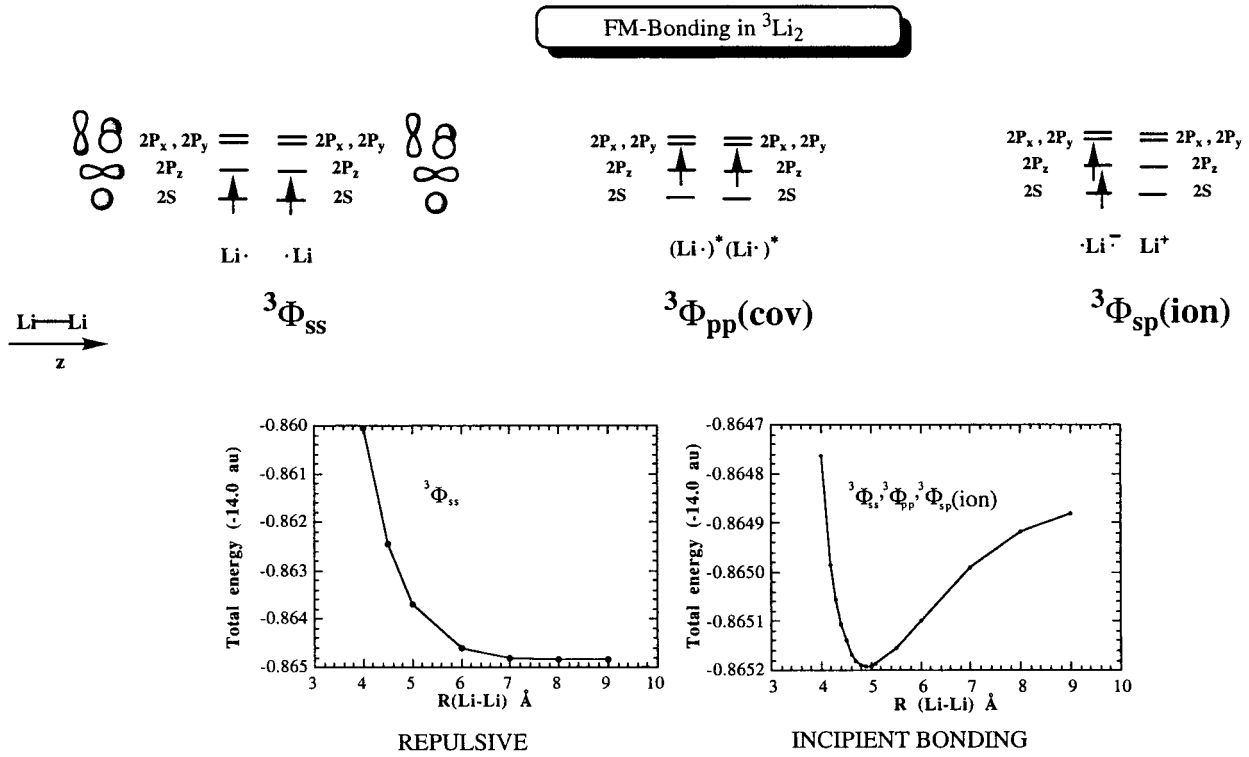

4.2. Origins of FM Bonding. In a recent paper,[10] we used BOVB calculations[25] to investigate the elementary FM bond of $^3Li_2$ ($^3\Sigma_u^+$). It was shown that the BDE could be reproduced at par with UCCSD(T) with three principal VB structures in Scheme 2. The fundamental structure, $^3\Phi_{ss}$, involves the triplet electrons in the 2s orbitals. The second structure is the covalent excited one, $^3\Phi_{pp}$, where the two 2s electrons are excited to the $2p_z$ orbitals. The third is one of the two ionic structures, where a 2s electron of one atom is transferred to the $2p_z$ orbital of the second atom. The reverse charge transfer generates the second ionic structure.

The energy curve of the fundamental structure is shown at the bottom of the scheme to exhibits a repulsive triplet interaction as might be expected from a triplet pair. However, the mixing of the locally excited structure, $^3\Phi_{pp}$, and especially the two corresponding charge-transfer structures, $^3\Phi_{sp}$(ion), lower the energy by adding resonance energy because of mixing. Now a minimum is created in the potential energy curve, and an incipient FM bond is thereby established. Of course this is due to the availability of low lying 2p orbitals on Li. However, this is not due to the simple s−p hybridization, because the HF wave function that involves significant s−p hybridization is not bound and so is the GVB wave function. The bonding requires the freedom of the multistructure covalent-ionic VB wave function. It follows therefore that *the FM bonding in the VB picture originates in the covalent-ionic fluctuations of the triplet electron pair*.

If the bonding picture in the dimer pertains also to the FM bonding in larger no-pair clusters, then it should be possible to project from the dimer and calculate the binding energy for the entire series of clusters. Thus, for a general no-pair cluster $^{n+1}Li_n$, there will be a fundamental 2s-only structure (i.e., $2s_1^1...2s_n^1$) which is repulsive. In addition there will exist a collection of excited covalent structures where two of the 2s electrons are replaced by $2p_\sigma$ electrons. In addition, there will be ionic structures, where one electron is transferred from a 2s orbital of one Li to a $2p_\sigma$ orbital of an adjacent Li. Because ionic configurations are high lying, we count only the mono-ionic structures, namely, those with a single Li^+ $^3Li^-$ pair in each structure. Furthermore, because the FM bonding is sensitive to distance, it is short-ranged, and therefore, we can keep only the monoionic and covalent excited structures with close-neighbor ion pairs and $2p_\sigma-2p_\sigma$ excited neighboring atoms. Thus, we have a collection of VB structures which, by mixing with each other, permit the $2p_\sigma-2p_\sigma$ excited and the $2s-2p_\sigma$ ionic pairs to propagate throughout the Li−Li neighbors in the cluster.

The contributions of ionic and covalent structures to the BDE of the dimer are known for the corresponding VB calculation.[10] These contributions are assumed to carry over to larger cluster, in a given distance r between the atoms. The stabilization energies because of the mixing of these configurations were shown[10] to obey perturbation theory, and therefore, the total FM bonding is a simple summation of the individual bonding contributions. Thus, if we count only close-neighbor 2s−2s repulsion ($\delta\epsilon_{rep}$) we can easily express the total repulsion energy in the 2s-only structure as a sum of close neighbor repulsion. Similarly, if we take a mixing increment, $\delta\epsilon_{mix}$, for each excited and ionic structures and assume for simplicity that these mixing terms are identical for the various VB structures, we can obtain the total resonance energy stabilization that is due to the VB mixing by simple counting of the excited and ionic VB structures. The total BDE can then be written[10,33] as the sum of repulsive and mixing energy terms, as follows in eq 1:

$$\mathrm{BDE_{FM}}(^{n+1}\mathrm{Li}_n) = -(3 + 4\sum_j C_j)\delta\epsilon_{\mathrm{mix}} - {}^1/_2\delta E_{\mathrm{rep}}\sum_j C_j \quad (1)$$

Here, C_j is the coordination number of atom j in the cluster. A simple expression of the bond energy per atom can be obtained if we take a uniform coordination number C. Then $\mathrm{BDE_{FM}}/n$

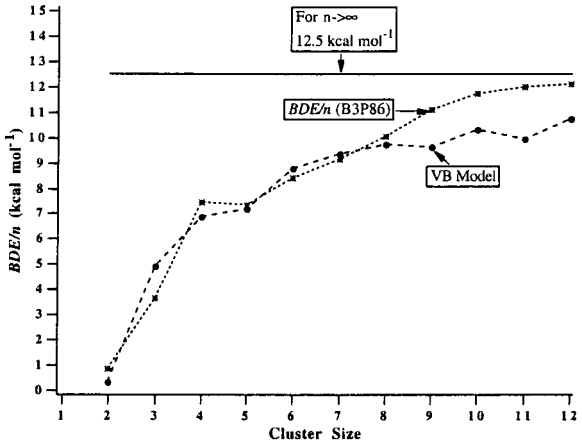

Figure 6. BDE/*n* values predicted by the VB model (eq 1) plotted vs the cluster size, *n*, along with the corresponding B3P86/cc-pVDZ values.

becomes

$$\mathrm{BDE_{FM}}/n = -4C\delta\epsilon_{\mathrm{mix}} - {}^1/_2 C\delta E_{\mathrm{rep}}\ (n \rightarrow \infty) \qquad (2)$$

This equation shows how the bond energy per atom depends crucially on the coordination number (*C*) of the atom. Equations 1 and 2 predict that the no-pair cluster will assume symmetric structures with uniform distances to minimize the pairwise 2s−2s repulsion and will attempt to maximize the atomic coordination number in order to maximize the mixing term. Thus, the equation gives a qualitatively reasonable description of the computed trends for the no-pair clusters as presented in Figure 5 and in Tables 1 and 2.

Let us turn now to a quantitative application of eq 1. On the basis of BOVB/cc-pVDZ calculations for $^3Li_2$, the repulsion and mixing parameters are $\delta E_{\mathrm{rep}} = 1.504$ kcal mol^{-1} and $\delta\epsilon_{\mathrm{mix}} = -0.7143$ kcal mol^{-1}.[10] Counting only the short distances in the coordination number of each atom in the clusters leads to the BDE and BDE/*n* values for any cluster based on eq 1. The results are plotted in Figure 6 against the cluster size *n*, alongside the B3P86 BDE/*n* value.

It is seen that the VB model is quite good. It predicts the order of magnitude of the BDE/*n* quantity, its steep initial rise as a function of *n*, and its convergence around $n = 10-11$. Moreover, by application to different isomers[34] for a given cluster size, the model equation predicts also the tendency of "no-pair" bonding to maximize the coordination number (C_j) and create "egg"-like structures. The individual VB values are a bit lower than the B3P86 values. No doubt the main reason for this quantitative deficiency is the neglect of higher ionic VB structures in the VB model.[34] Nevertheless, the quantitative deviations are not too significant, and the VB model seems to capture the essence of FM bonding. Thus, the FM bonding, of a given atom with coordination number *C* (eq 2), is a collective resonance energy, endowed by the mixing of all possible pairwise locally excited and ionic structures into the $2s^12s^1$ pairs the atom shares with the neighbors in its coordination shell. FM bonding of a given atom is caused then by the covalent−ionic fluctuations of all of the triplet pairs that this atom maintains with its close neighbors. This covalent−ionic fluctuation propagates over the entire cluster across all the short Li−Li contacts that emanate from a single atom, thereby leading to a delocalized FM bonding.

Orbital Cartoon Model of FM Bonds. To render the notion of FM bonding qualitatively communicable we must seek an orbital picture that is in harmony with the VB model. This means that the orbital picture should correspond to a two-center FM bond that undergoes delocalization over all the short Li−Li distances in the cluster. Our starting point is the $^3Li_2$ cluster in its ferromagnetic state of $^3\Sigma_u^+$ symmetry, which is expressed as a linear combination of the main VB structures discussed above in Scheme 2.

An orbital picture can be achieved by grouping the linear combination of these VB structures into a more compact wave function that contains hybridized and semilocalized atomic orbitals. The wave function is dominated by the fundamental structure, $^3\Phi_{ss}$, and has smaller but significant contributions of the excited covalent structure, $^3\Phi_{pp}$(cov), and the ionic structures, $^3\Phi_{sp}$(ion). To have a better appreciation of the individual effects of $^3\Phi_{pp}$(cov) and $^3\Phi_{sp}$(ion), on the fundamental structure, $^3\Phi_{ss}$, we shall carry out the procedure in two steps.

When we start with the combination of $^3\Phi_{ss}$ and $^3\Phi_{pp}$(cov), a wave function, with the proper $^3\Sigma_u^+$ symmetry, can be rewritten as follows (dropping normalization constants in the Slater determinants here and elsewhere):

$$^3\Phi_{ss} + c\,^3\Phi_{pp} = |(2s_1 + \lambda 2p_1)(2s_2 + \lambda 2p_2)| + |(2s_1 - \lambda 2p_1)(2s_2 - \lambda 2p_2)|; \quad c = \lambda^2 \qquad (3)$$

The wave function is seen to involve a resonating mixture of two structures with orbitals, which are hybrids of the 2s and $2p_z$ AOs on the same center. This wave function and the hybrid orbitals are depicted (using $\lambda = 0.30$) in Scheme 3a. For comparison, we show also the fundamental structure $^3\Phi_{ss}$ in Scheme 3b. It is seen that in each one of the structures in Scheme 3a the triplet pair of electrons occupy an "in−out" or an "out−in" pair of hybrids, such that the average distance of the electron pair increases. This is a simple expression of the fact that the $^3\Phi_{pp}$(cov) structure tries to mitigate the triplet repulsion of the electron pair in the 2s orbitals of the $^3\Phi_{ss}$ structure.

Adding now the ionic structures to the wave function in eq 3 leads to the ferromagnetic bond (FM) wave function that is expressed in eq 4:

$$\Phi_{FM}(^3\Sigma^+_u) = |(2s_1 + \lambda 2p_1)(2s_2 + \lambda 2p_2 - \lambda 2p_1)| + |(2s_1 - \lambda 2p_1 + \lambda 2p_2)(2s_2 - \lambda 2p_2)| \qquad (4)$$

Thus, the ionic structures mix to bring in some charge shift bonding, because of covalent−ionic resonance, and retain the "in−out" ↔ "out−in" pattern of the constituent orbitals. The charge shift bonding is associated with the delocalization tails, which are seen in eq 4 to develop in only one of the orbitals in each of the two VB structures. A plot of one of these semidelocalized hybrids is shown in Scheme 3c (using $\lambda = 0.30$). This delocalization of the "in-out" hybrids endows the $^3Li_2$ cluster with a charge-shift resonance energy and stabilizes the FM bond relative to the dissociated atoms. We may therefore conclude that FM bonding is sustained by the charge shift resonance energy because of the covalent−ionic fluctuation of the triplet pair that resides in "in−out" hybridized orbitals.

Inspection of the hybrid that carries a delocalization tail, in Scheme 3c, shows that it involves an interstitial density, in a manner reminiscent of the McAdon−Goddard interstitial bonding in ground-state Li clusters.[16−18] In fact, by starting with interstitial orbitals, the charge shift resonance energy is already embedded into the orbital energy, so that the two pictures have this feature in common although they may look different. The failure of the GVB wave function to give a bound the $^3Li_2$-($^3\Sigma_u^+$) and its underestimation of the binding energy for $^4Li_3$

SCHEME 3: Orbital Model of FM Bonding in $^3Li_2$: The Resonance of Two Structures with In−Out and Out−In Hybrids (in a) Vis-à-Vis the Repulsive 2s−2s Triplet Pair (in b) and the In−Out ↔ Out−In Resonance in (a) Augmented by Charge-Shift Resonance Energy through the Delocalization Tails of the Hybrids (in c)

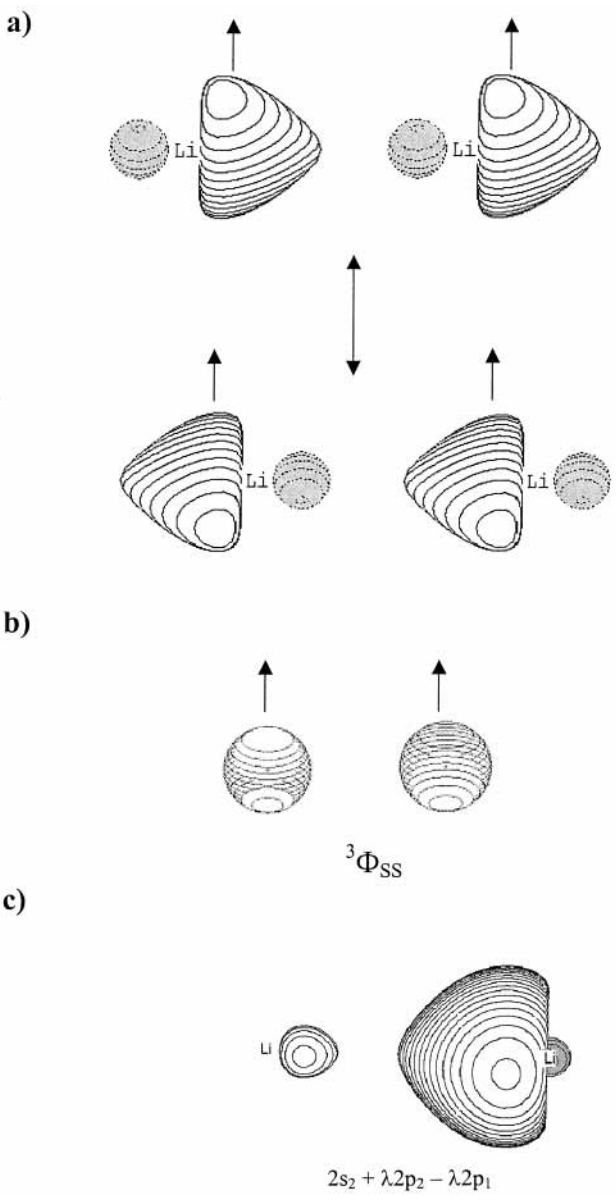

arise because GVB uses a single structure to describe this high-spin situation, whereas the bonding comes from a resonating wave function.

To extend the orbital cartoon to larger clusters, we consider the simplest polyatomic cluster, $^4Li_3$ in Scheme 4. We now have three resonance structures, $\mathbf{R_1}-\mathbf{R_3}$, which can delocalize the FM bond over the three possible Li−Li linkages (a−c). The FM bonds are represented by in−out hybrids, whereas the delocalization tails are not shown for simplicity. Consider first the situation in the linear structure as depicted in Scheme 4a. It is apparent that the structures $\mathbf{R_1}$ and $\mathbf{R_2}$ represent short FM bonds in mutual resonance, whereas the third structure, $\mathbf{R_3}$, has the FM bond localized in the long linkage (c). Consequently, the first two structures can mix efficiently and contribute to the overall FM bonding, whereas the third structure cannot mix with them efficiently and does not contribute therefore to the resonance energy stabilization of the FM bonding. To increase

SCHEME 4: R1, R2, and R3 which Are the VB Structures Required to Describe FM Bonding in $^4Li_3$, where the Most Stable Geometry Is an Equilateral Triangle in Which the Structures Mix Efficiently and Form Delocalized FM Bonding

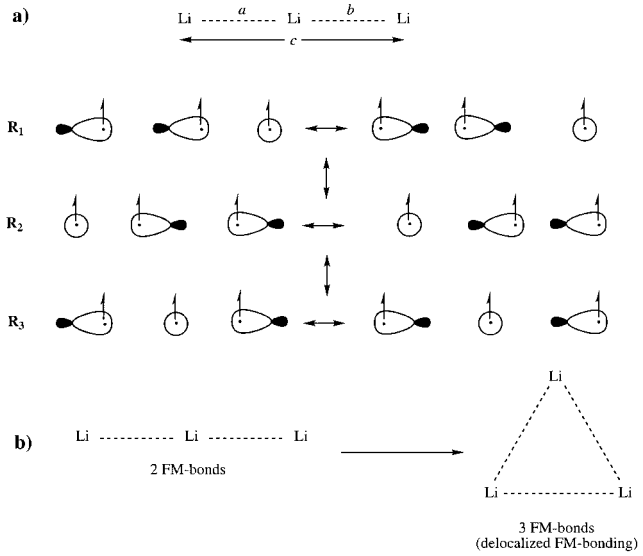

the FM bonding, $^4Li_3$ will assume the maximum possible coordination number in an equilateral triangular structure, Scheme 4b. Now, the FM bonding is fully delocalized, and each of the three structures contributes to charge shift bonding. Indeed, as predicted by eq 1, the BDE of the linear $^4Li_3$ species is 7.0 kcal mol^{-1}, whereas that for the equilateral triangle it is 14.7 kcal mol^{-1}.

From the example of the $^4Li_3$ species, we can make generalizations about FM bonding. The delocalized FM bonding arises by spreading the covalent−ionic fluctuation of the FM pair hybrids over all the available short Li−Li linkages in the cluster. It is apparent that, because the elementary FM pair is weakly bound, the more structures that are available to delocalize the fluctuation, the stronger the FM bonding will be. Consequently, it is crucially important that each Li atom in the cluster will possess the highest possible coordination number and, thereby, maximize the number of its FM bonds. This is the origins of the "egg"-like structures which were produced by DFT calculations and displayed in Figure 5, and this is the origins of the bonding patterns in Tables 1 and 2, which show that the smaller the coordination number of Li, the weaker the FM bonding.

5. Conclusion and Summary

Using DFT calculations, we generated a family of the high spin lithium clusters $^{n+1}Li_n$ ($n = 2-12$), which do not possess any electron pairs but which are nevertheless strongly bound.[9−11] The B3P86 bonding energy was found to rise steeply from 1.7 kcal mol^{-1} for the dimer to 145 kcal mol^{-1} for the dodecamer (the corresponding B3PW91 data are 0.85 and 134 kcal mol^{-1}). The bond energy per atom, BDE/*n*, converges for cluster sizes of $n = 11-12$ and reaches 11−12 kcal/mol. With such strength, the bonding in these clusters is termed FM bonding. It is found that FM bonding prefers highly symmetrical egg-shaped structures with a high coordination number for the Li atom.

We addressed here the origins and properties of FM bonding using a VB model, on the basis of previous detailed calculations of the $^3Li_2$ dimer.[10] The dimer is bonded because of the covalent−ionic fluctuation of the triplet pair. In VB terms, this

arises as the excited covalent structure, $^3\Phi_{pp}$(cov) (with occupancy in the $2p_z$ orbitals), and the ionic structures, $^3\Phi_{sp}$(ion), mix with the intrinsically repulsive fundamental structure, $^3\Phi_{ss}$ (with 2s-only occupancy), Scheme 2. On the basis of the results of the dimer, a simple VB model equation is constructed (eq 1) that allows for the estimation of the FM bonding energy for any cluster size. The VB model predicts quantitatively the bonding energies, and the convergence of bonding energy per atom (BDE/*n*) at $n = 11-12$, and the root cause of the structural preference.

An orbital cartoon for this bonding is proposed on the basis of the computed VB wave function of the $^3Li_2$ dimer. In this orbital picture of the FM pair (Scheme 3), there are two resonance structures, one with hybrids which point "in−out" and the other with "out−in". This unique hybridization keeps the triplet electrons apart and thereby mitigates their repulsion. In addition, the hybrids possess delocalization tails, which account for the mixing of the ionic structures, and these tails bring in charge-shift resonance energy that stabilizes the FM pair below the energy of the dissociated atoms.

Simple arguments show how to extend the picture to larger clusters. In these cases, every short Li−Li linkage is allowed to assume the unique orbitals of the FM pair, and the wave function is a resonating mixture of all possible pairs. Because the elementary FM pair is weak, it is crucially important that each Li atom in the cluster will possess the highest possible coordination number, to maximize thereby the number of its FM bonds. Thus, the shape of the cluster and its steeply rising bond energy as well as the convergence of the bonding energy of a given atom all find a simple rationale in the VB model.

It must be recalled that these no-pair clusters are excited states of the corresponding low-spin states. Nevertheless, the strength of FM bonding and the high-spin state of the clusters suggest that these species, of maximum magneticity, will have sufficiently long lifetime to be observed by experimental means. The observation of the $^3Cs_2$,[12] by means of photoassociation spectroscopy, gives hope that larger clusters can be generated and probed, e.g., in combination with the technique used in the classical Stern−Gerlach experiment.

In conclusion then, *FM bonding is a delocalized covalent−ionic fluctuation that spreads over the entire cluster*. This bonding type is likely to manifest in all of the noble elements (Ag, Cu, and Au) as well as in elements of group III. FM bonding may turn out to be a generally useful paradigm of bonding.

Acknowledgment. The authors thank the Robert Szold Fund and the Niedersachsen Foundation for support.

Supporting Information Available: Six tables (S1−S6) with absolute and relative energies and six Figures (S1−S6) with all optimized structures are available. This material is available free of charge via the Internet at http://pubs.acs.org.

References and Notes

(1) Bonacic-Koutecky, V.; Fantucci, P.; Koutecky, J. *Chem. Rev.* **1991**, *91*, 1035.

(2) Gerber, G. B.; McCoy, A. B.; Garcia-Vela, A. *Annu. Rev. Phys. Chem.* **1994**, *45*, 275.

(3) Castleman, A. W., Jr.; Wei, S. *Annu. Rev. Phys. Chem.* **1994**, *45*, 685.

(4) Buck, U. *Adv. Mol. Opt. Phys.* **1995**, *35*, 121.

(5) Special Issue in *Science* **1996**, *271*, Edited by Brauman, J. I.

(6) Castleman, A. W., Jr.; Bowen, K. H., Jr. *J. Phys. Chem.* **1996**, *100*, 12911.

(7) Bacic, Z.; Miller, R. E. *J. Phys. Chem.* **1996**, *100*, 12945.

(8) Rousseau, R.; Marx, D. *Chem. Eur. J.* **2000**, *6*, 2982.

(9) Glukhovtsev, M. N.; von Ragué Schleyer, P. *Isr. J. Chem.* **1993**, *33*, 455.

(10) Danovich, D.; Wu, W.; Shaik, S. *J. Am. Chem. Soc.* **1999**, *121*, 3165.

(11) de Visser, S. P.; Alpert, Y.; Danovich, D.; Shaik, S. *J. Phys. Chem. A* **2000**, *104*, 11223.

(12) Fiortti, A.; Comparati, D.; Crubelier, A.; Dulieu, O.; Mansou-Seeuws, F.; Pillet, P. *Phys. Rev. Lett.* **1998**, *80*, 4402.

(13) Boustani, L.; Pewestorf, W.; Fantucci, P.; Bonacic-Koutecky, V.; Koutecky, J. *Phys. Rev. B* **1987**, *35*, 9437.

(14) Rao, B. K.; Khanna, S. N.; Jena, P. *Phys. Rev. B* **1987**, *36*, 953.

(15) Förner, W.; Seel, M. *J. Chem. Phys.* **1987**, *87*, 443.

(16) McAdon, M. H.; Goddard, W. A., III. *J. Phys. Chem.* **1987**, *91*, 2607.

(17) McAdon, M. H.; Goddard, W. A., III. *J. Chem. Phys.* **1987**, *88*, 277.

(18) McAdon, M. H.; Goddard, W. A., III. *J. Phys. Chem.* **1988**, *92*, 1352.

(19) Blanc, J.; Bonacic-Koutecky, V.; Broyer, M.; Chevaleyre, J.; Dugourd, Ph.; Koutecky, J.; Scheuch, C.; Wolf, J. P.; Wöste, L. *J. Chem. Phys.* **1992**, *96*, 1793.

(20) Jellinek, J.; Bonacic-Koutecky, V.; Fantucci, P.; Wiechert, M. *J. Chem. Phys.* **1994**, *101*, 10092.

(21) Gardet, G.; Rogemond, F.; Chermette, H. *J. Chem. Phys.* **1996**, *105*, 9933.

(22) Jones, R. O.; Lichtenstein, A. I.; Hutter, J. *J. Chem. Phys.* **1997**, *106*, 4566.

(23) Reichardt, D.; Bonacic-Koutecky, V.; Fantucci, P.; Jellinek, J. *Chem. Phys. Lett.* **1997**, *279*, 129.

(24) Jellinek, J.; Srinivas, S.; Fantucci, P. *Chem. Phys. Lett.* **1998**, *288*, 705.

(25) Hiberty, P. C.; Humbel, S.; Byrman, C. P.; van Lenthe, J. H.; *J. Chem. Phys.* **1994**, *101*, 5969. Hiberty, P. C.; Humbel, S.; Archirel, P. *J. Phys. Chem.* **1994**, *98*, 11697.

(26) Frisch, M. J.; Trucks, G. W.; Schlegel, H. B.; Scuseria, G. E.; Robb, M. A.; Cheeseman, J. R.; Zakrzewski, V. G.; Montgomery, J. A., Jr.; Stratmann, R. E.; Burant, J. C.; Dapprich, S.; Millam, J. M.; Daniels, A. D.; Kudin, K. N.; Strain, M. C.; Farkas, O.; Tomasi, J.; Barone, V.; Cossi, M.; Cammi, R.; Mennucci, B.; Pomelli, C.; Adamo, C.; Clifford, S.; Ochterski, J.; Petersson, G. A.; Ayala, P. Y.; Cui, Q.; Morokuma, K.; Malick, D. K.; Rabuck, A. D.; Raghavachari, K.; Foresman, J. B.; Cioslowski, J.; Ortiz, J. V.; Stefanov, B. B.; Liu, G.; Liashenko, A.; Piskorz, P.; Komaromi, I.; Gomperts, R.; Martin, R. L.; Fox, D. J.; Keith, T.; Al-Laham, M. A.; Peng, C. Y.; Nanayakkara, A.; Gonzalez, C.; Challacombe, M.; Gill, P. M. W.; Johnson, B. G.; Chen, W.; Wong, M. W.; Andres, J. L.; Head-Gordon, M.; Replogle, E. S.; Pople, J. A. *Gaussian 98*, revision A.9; Gaussian, Inc.: Pittsburgh, PA, 1998.

(27) Becke, A. D. *J. Chem. Phys.* **1993**, *98*, 5648.

(28) Perdew, J. P. *Phys. Rev. B* **1986**, *33*, 8822.

(29) Perdew, J. P.; Wang, Y. *Phys. Rev. B* **1992**, *45*, 13244.

(30) Dunning, T. H., Jr. *J. Chem. Phys.* **1989**, *90*, 1007.

(31) Woon, D. E.; Dunning, T. H., Jr. *J. Chem. Phys.* **1993**, *98*, 1358.

(32) Woon, D. E. private communication.

(33) The original equation in ref 10 did not include the covalent structures which are obtained from the fundamental one by pair wise $2s_i2s_j \rightarrow 2p_i2p_j$ excitations. The difference is in the value of the multiplier 4 instead of 3 in eq 1.

(34) The model predicts the inferiority of the cyclic and linear structures compared with the maximally coordinated clusters. Inclusion of di-ionic structures has a negligible effect on the maximally coordinated clusters but it improves the quantitative estimate of the BDE/n for the cyclic and linear structure. Thus, a plot of BDE/n(B3P86) − BDE/n (eq 1) against the number of di-ionic converges properly and predicts an asymptotic value of BDE/n = 8 kcal mol^{-1}. The important di-ionic structures are those with charge alternation. These structures are low in energy for cyclic (and linear) isomers but get destabilized in the three-dimensional isomers because of the repulsion of like charges. The best way to understand that is to look at the alternate di-ionic structure of a planar $^5Li_4$ and how it gets destabilized when the cluster becomes tetrahedral.